International Journal of Mass Spectrometry 285 (2009) 143–148

Contents lists available at ScienceDirect

International Journal of Mass Spectrometry

journal homepage: www.elsevier.com/locate/ijms

Microscopic studies of atom–water collisions

Z.P. Wang[a,b,h], P.M. Dinh[a,b], P.-G. Reinhard[c], E. Suraud[a,b], G. Bruny[d,e,f], C. Montano[d,e,f], S. Feil[d,e,f], S. Eden[d,e,f,1], H. Abdoul-Carime[d,e,f], B. Farizon[d,e,f,*], M. Farizon[d,e,f], S. Ouaskit[d,e,f,2], T.D. Märk[g]

[a] Université de Toulouse; UPS; Laboratoire de Physique Théorique (IRSAMC), F-31062 Toulouse, France
[b] CNRS; LPT (IRSAMC), F-31062 Toulouse, France
[c] Institut für Theoretische Physik, Universität Erlangen, D-91058 Erlangen, Germany
[d] Université de Lyon, F-69003, Lyon, France
[e] Université Lyon 1, Villeurbanne, France
[f] CNRS/IN2P3, UMR5822, Institut de Physique Nucléaire de Lyon; F-69622 Villeurbanne, France
[g] Institut für Ionenphysik und Angewandte Physik, Leopold Franzens Universität, Technikerstrasse 25, A-6020 Innsbruck, Austria
[h] The Key Laboratory of Beam Technology and Material Modification of Ministry of Education, College of Nuclear Science and Technology, Beijing Normal University, Beijing 100875, People's Republic of China

ARTICLE INFO

Article history:
Received 31 March 2009
Received in revised form 25 May 2009
Accepted 25 May 2009
Available online 6 June 2009

Keywords:
Water clusters
Collision dynamics
Collision induced dissociation
Collision induced ionization

ABSTRACT

The influences of water molecules surrounding biological molecules during irradiation with heavy particles (atoms, ions) are currently a major subject in radiation science on a molecular level. In order to elucidate the underlying complex reaction mechanisms, we have initiated a joint experimental and theoretical investigation with the aim to make direct comparisons between experimental and theoretical results. As a first step, studies of collisions of a water molecule with a neutral projectile (C atom) at high velocities ($\geq$0.1 a.u.), and with a charged projectile (proton) at low velocities ($\leq$0.1 a.u.) have been studied within the microscopic framework. In particular, time-dependent density functional theory (TDDFT) was applied to the valence electrons and coupled non-adiabatically to molecular dynamics (MD) for ionic cores. Complementary experimental developments have been carried out to study projectile interactions with accelerated ($\leq$10 keV) and mass-selected cluster ions. The first size distributions of protonated water cluster ions $H^+(H_2O)_n$ (n = 2–39) produced using this new apparatus are presented.

1. Introduction

While the use of ionizing radiation is well-established, notably in therapies and analytical techniques, each new development opens a field of investigation around the possible dangers to our health and the environment [1,2]. Concurrently, besides applications and risk evaluations, the effect of ionizing radiation in biomolecular nanosystems is emerging as a major area of research, both on a fundamental level and as a source for experimental and technical innovations. The irradiation of biomolecular nanosystems in the gas phase under single collision conditions represents a significant new subject in radiation science. From an experimental standpoint, it has great potential for the development of new analytical techniques and synthesis techniques. Complementary theoretical progress can provide new descriptions of radiative energy transfer mechanisms on the molecular scale, opening new perspectives for the elucidation of the radiation dose in living systems.

Our principle goal is to investigate microscopic mechanisms responsible for irradiation effects in biological molecules with a particular focus on the influence of water molecules in the environment of these molecules. This is achieved here in a joined experimental and theoretical effort with the aim to make direct comparisons between experimental and theoretical results. The originality of this work lies in the ability to quantify the role of a biomolecule's immediate environment in proton radiation-induced processes through the precise control of the number of associated water molecules. This is a key aspect from the fundamental physics point of view and it is also crucial to allow realistic and detailed comparisons between experiments and theory. The path towards such an ambitious goal is long and, due to the many elementary processes involved, one needs to validate the various experimental and theoretical aspects. First of all, we consider here the simplest case of a single water molecule interacting with a projectile, which constitutes a prerequisite for any further developments. The next step involving an assembly of water molecules around a biomolecule raises no major theoretical difficulty because the number of molecules can be efficiently controlled.

* Corresponding author.
E-mail address: bfarizon@ipnl.in2p3.fr (B. Farizon).
[1] Present address: Department of Physics and Astronomy, The Open University (OU), Walton hall, Milton Keynes MK76AA, UK.
[2] Present address: Université Hassan II-Mohammedia, Faculté des Sciences Ben M'Sik (LPMC), B.P.7955 Ben M'Sik, Casablanca, Morocco.

1387-3806/$ – see front matter © 2009 Elsevier B.V. All rights reserved.
doi:10.1016/j.ijms.2009.05.008

Monitoring this number experimentally constitutes a key issue for further experimental developments and for comparisons with theory.

In previous experiments at the Institut de Physique Nucléaire de Lyon, the ionization of gas-phase water molecules by protons [3] and neutral hydrogen [5] impact has been studied in the velocity range of 0.9–2.5 a.u.(units of the Bohr velocity), coinciding with the Bragg peak maximum for energy deposition by an ion beam in an absorbing medium. Mass-analyzed $H_2O^+$and fragment ions of the water molecules were detected in coincidence with the projectile following ionization in single collision conditions. The determination of the charge state of the projectile after the collision enabled ionization processes to be separated on the basis of charge transfer between the target molecule and the projectile. Thus it was possible to measure branching ratios and absolute cross sections for water ionization with and without the capture of an electron by the incident proton.

The present experimental challenge is to study interactions between water molecules in a cluster following 0.9–2.5 a.u. proton impact induced excitation/ionization of water prior to dissociation. Accordingly, a new experimental system has been developed to investigate the proton irradiation of mass-selected protonated water clusters. Many different techniques have been used successfully to generate ensembles of water cluster ions including electrospray ionization [6,7], electron impact ionization [8], corona discharge ionization [8], chemical ionization [9] and electrospray droplet impact [10,11]. The novelty of the present experimental system lies in the acceleration (up to 10 kV) and mass-selection of molecular and cluster ions of water prior to 0.9–2.5 a.u. collisions with protons.

The microscopic description of radiation-induced processes requires an explicit dynamical account of electronic degrees of freedom which respond first in the present collisions. Moreover, it is necessary to treat electrons in a non-adiabatic way and to allow for ionization and/or electron transport. This invalidates most calculations based on the Born-Oppenheimer (BO) approximation except in some specific situations. Indeed, depending on the characteristics of the ionizing projectile (charge, velocity), one can treat the problem in a simplified manner by decoupling electronic and ionic dynamics. A typical example is the case of high velocity charged projectiles in which ions can be safely considered as frozen and the dynamics reduced to the electronic response, at least for short times. Another example is the case of low velocity neutral projectiles for which a ground state (BO) treatment is acceptable. To the best of our knowledge, low velocity charged and high velocity neutral projectiles can nevertheless not be treated by the usually available calculations [12], and certainly not in the framework of a unique theoretical approach [13]. Fortunately, in the case of cluster dynamics, several approaches [14–16,22,23] have been developed which consider this question of coupled electronic and ionic dynamics in relation to irradiation by intense laser fields. A coupling of the optically active spot to a large environment can be added in a hierarchical approach [24,25]. In the present work, we have adapted the non-adiabatic approach of Calvayrac et al. [16], originally developed for metal clusters, to the case of an organic molecule and applied it to realistic irradiation scenarios. The method of Calvayrac et al. [16] contains as limiting cases pure electron dynamics and BO dynamics (Car-Parinello dynamics) and can thus describe collisions with high-velocity charged or low-velocity neutral projectiles. Moreover, at variance with currently available approaches, it enables complementing cases to be described such as low-velocity charged and high-velocity neutral projectiles. Indeed such a non-adiabatic approach places no restriction on the velocity or charge state of the projectile and thus offers an unified picture of many possible irradiation scenarios.

2. Experimental set up

We briefly present the experimental system in this section. The experimental set up will be thoroughly described elsewhere [4]. All measurements are taken with a two-sector-field mass spectrometer of EB geometry combined with an electron-impact ion source. Neutral clusters are produced by expanding water vapor from a stagnation chamber at a temperature of around 100 °C and a pressure of approximately 1 bar through a pin-hole nozzle (20 μm diameter) into vacuum. In this isentropic expansion, the temperature drops rapidly with increasing distance from the nozzle leading to super-saturation of the water vapor and subsequent clustering. The clusters are ionized by electrons of 50 eV (experimentally available range from about 0–50 eV) and the pressure in this region is maintained at 2×10^{-4} mbar by a 1200 L/s oil diffusion pump. The resulting positive ions and cluster ions (charge state q) are immediately extracted from the center of the ion source by a weak penetrating electric field. The extracted ions pass through a skimmer and are accelerated to $(6 \times q)$ keV. An Einzel lens and four pairs of deflection plates are used to direct the beam to the focal point of a hemispherical electric sector field with maximum transmission. The electric sector field serves to select ions according to their kinetic energy, thus increasing the energy resolution of the beam. The kinetic energy resolved ion beam then passes through a magnetic sector field for ion selection according to momentum. Finally, the mass-selected water cluster ions $H^+(H_2O)_n$are focused into the *collision chamber*and detected through a 1 mm collimator by a channeltron electron multiplier operated in a counting mode. Further experimental developments are currently being carried out in order to intersect the cluster ion beam with an intense beam of 0.9–2.5 a.u. protons or a jet of atomic or molecular gas (He, N_2, etc.).

3. Theoretical methods

In order to perform microscopic simulations of dynamical processes, we employ time-dependent density functional theory (TDDFT) [17] for the electrons combined with classical molecular dynamics (MD) for the ionic cores. More precisely, the degrees of freedom of the model are the wave functions of valence electrons of the system, $\{\varphi_\alpha(\mathbf{r}), \alpha = 1 \ldots N_{\mathrm{el}}\}$, and the coordinates of the system's ionic cores, $\{\mathbf{R}_I, I = 1 \ldots N_{\mathrm{ion}}\}$. In this letter, the various ions can be H^+, C^{4+}, and O^{6+}. One starts from the total energy of the system E_{tot}:

$$E_{\mathrm{tot}} = E_{\mathrm{kin}}(\{\varphi_\alpha\}) + E_{\mathrm{C}} + E_{\mathrm{xc}} + E_{\mathrm{el,ion}}(\rho, \{\mathbf{R}_I\}) + E_{\mathrm{ext}}(\rho, \{\mathbf{R}_I\}, t). \quad (1)$$

The electronic density is defined as $\rho = \sum_\alpha |\varphi_\alpha|^2$. The various contributions to the E_{tot} in Eq. (1) are successively the electron kinetic energy, the direct Coulomb energy, the exchange-correlation energy, the coupling energy between electrons and ions, and the energy coming from the interaction of the system with an external time-dependent field (that of a by-passing atom or ion here). The functional E_{xc} used for the exchange-correlation energy is from Perdew and Wang [18].

Equations of motion are then derived in a standard manner by variation of E_{tot}. On one hand, variation with respect to φ_α^* leads to the (time-dependent) Kohn–Sham equations for the single-particle wave functions,

$$i\hbar \frac{\partial}{\partial t}\varphi_\alpha = \hat{h}_{\mathrm{KS}}\varphi_\alpha, \quad (2a)$$

$$\hat{h}_{\mathrm{KS}} = \frac{\hat{p}^2}{2m_e} + V_{\mathrm{C}} + V_{\mathrm{xc}} + V_{\mathrm{PsP}} + V_{\mathrm{ext}}^{\mathrm{el}}. \quad (2b)$$

The coupling between electrons and ionic cores is treated via a pseudopotential V_{PSP} and is detailed below.

On the other hand, Hamiltonian equations of motion for ions, thus treated by classical MD, are derived by variation with respect to $\mathbf{R}_I$ and $\mathbf{P}_I$ and read

$$\frac{\partial}{\partial t}\mathbf{R}_I = \frac{\mathbf{P}_I}{M_I}, \tag{3a}$$

$$\frac{\partial}{\partial t}\mathbf{P}_I = -\nabla_{\mathbf{R}_I}\left[\sum_{I\neq J}\frac{Z_I Z_J\, e^2}{|\mathbf{R}_I-\mathbf{R}_J|} + \sum_{\alpha=1}^{N_{el}}\langle\varphi_\alpha|V_{PsP}(\mathbf{r}-\mathbf{R}_I)|\varphi_\alpha\rangle + V_{ext}^{ion}\right]. \tag{3b}$$

In the last equation, Z_I and M_I stand for the charge and the mass of ionic core I, and V_{ext}^{ion} the coupling potential of ions with the external field.

Since Eqs. (2) and (3) are computed and solved simultaneously, both electrons and ions are fully propagated in time. One can recover two limiting cases from this approach: (i) pure electronic motion with a frozen ionic geometry [TDDFT only, Eqs. (2)] [12], and (ii) BO dynamics where ions are propagated in time, Eqs. (3), while electrons are in their ground-state (obtained by standard static DFT methods) [12,19]. The power of our method, coupling TDDFT and MD, is to provide the non-adiabatic dynamics of the system, which can reduce to an adiabatic description if the ionic motion is slow enough to allow electrons to relax in their ground-state.

TDDFT is used at the level of the local-density approximation (LDA) [20,21] together with an average-density self-interaction correction (ADSIC) [27] for the Coulomb and the exchange-correlation potentials in Eq. (3b). This allows us to achieve the correct ionization potentials, a feature which is crucial to describe electron emission correctly, especially close to threshold.

Time-dependent fields and wave functions are represented on a 3D coordinate-space grid of dimensions $72 \times 72 \times 64$. Electronic wave functions are propagated in time by the time-splitting method [29]. The Poisson equation is evaluated by a fast Fourier technique [30]. Ionic equations of motion are solved using the Verlet algorithm. Absorbing boundary conditions are used to remove outgoing electrons. Thus the total number of electrons $N = N(t)$ decreases in time. The number of escaped electrons $N_{esc} = N(t=0) - N(t)$ is a measure of average ionization. The details of this method are presented elsewhere (e.g. [16,26]).

The coupling between electrons and ionic cores is achieved by Goedecker-type [28] pseudopotentials consisting of a local part and a non-local one, that is, for a given wave function φ_α:

$$V_{PsP}(r)\varphi_\alpha(r) = V_{loc}(r)\varphi_\alpha(r) + \int dr' V_{nloc}(r,r')\varphi_\alpha(r'), \tag{4a}$$

$$V_{loc}(r) = -\frac{Z_I}{r}\,\mathrm{erf}\left(\frac{x}{\sqrt{2}}\right) + e^{-x^2/2}[C_1 + C_2\,x^2], \tag{4b}$$

$$V_{nloc}(r,r') = \sum_m Y_{0m}(\hat{r})p(r)h_0 p(r')Y_{0m}^*(\hat{r}'). \tag{4c}$$

In the local term, $x = r/r_{loc}$ and erf is the error function; in the non-local part, $Y_{0,m}$ denotes the spherical harmonic and $p(r)$ the following radial projector

$$p(r) = \frac{\sqrt{2}}{r_{nloc}^{3/2}\sqrt{\Gamma(3/2)}}\exp\left(-\frac{r^2}{2r_{nloc}^2}\right). \tag{4d}$$

The original parameterizations employ different Gaussian widths r_{loc} and r_{nloc} for each material and contribution. This hampers numerical precision in coordinate space grids. We have refitted new pseudopotential parameters (that is C_1, C_2 and h_0) for the smallest width of $0.412a_0$ in all terms (local and non-local) and for all elements involved in the study. Further details will be given in a forthcoming publication.

4. First results

4.1. Experimental production of size resolved protonated water clusters

Fig. 1 shows a typical mass spectrum obtained for the water cluster beam by scanning the magnetic sector field. This spectrum was recorded for an acceleration voltage of 6 kV and for a water vapor pressure and temperature of 1.1 bar and 100 °C in the stagnation chamber, respectively. The water monomer ion peak is not shown in the spectrum as its intensity is too high leading to saturation of the channeltron detector. The observed series of peaks spaced by 18 amu/unit charge is attributed to protonated water clusters comprising n molecules (n = 2–39). Water cluster ion intensities decrease exponentially (red dashed line in Fig. 1) as the number of water molecules increases. The other peaks correspond to components arising from the residual gas in the cluster source. The insert in the top panel of Fig. 1 shows the higher-mass peaks ($n = 18-39$) in greater detail. These peaks correspond to $H^+(H_2O)_n$, n = 18-39, cluster ions. The present size distribution of cluster ions is rather similar to that observed by Castleman and co-workers [9]. The present results are also plotted in the bottom panel of Fig. 1on a logarithmic scale. In this case, a clear drop in intensity can be seen for ion production above cluster size $n = 21$. This is consistent with previous results [9] supporting a *magic number* (that is, a particularly stable configuration) at this cluster size.

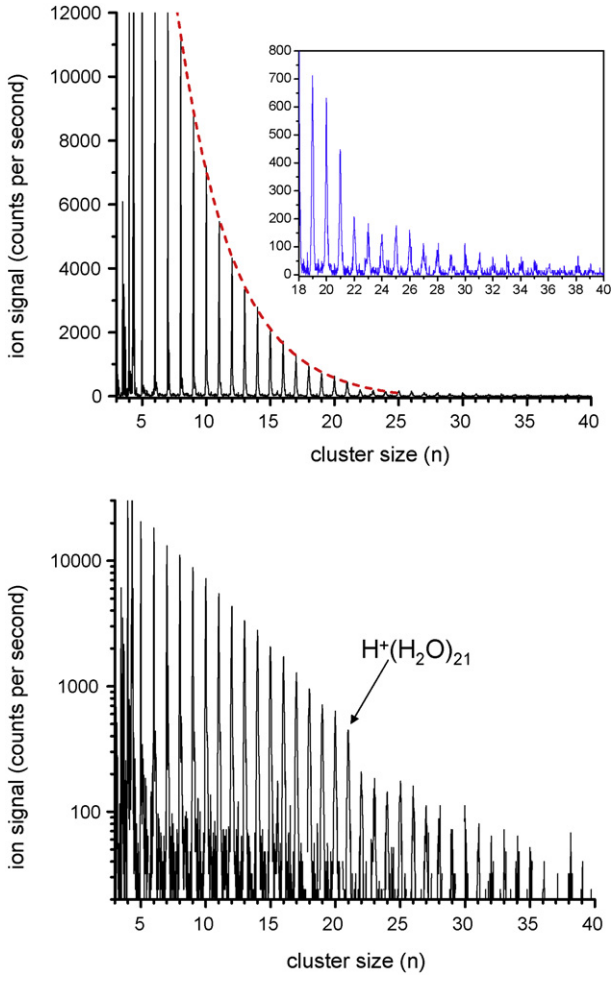

Fig. 1. *Top:* Spectrum of accelerated (6 keV) and mass-selected water cluster ions obtained by scanning the magnetic sector field. *Bottom:* Same in a logarithmic scale.

Importantly for our future experiments, the intensity of the mass-analyzed cluster ion beams achieved with the present set-up is rather high. For instance, the intensity of the protonated water trimer beam measured through the 1 mm-collimated channeltron is 5000 counts/s. In a next step, these mass selected cluster ion beams will be crossed by an intense proton beam and the resulting collision events will be analyzed using a molecular imaging detection system.

4.2. Theoretical studies of the irradiation of water molecules

As discussed in Section 1, the ultimate aim of our combined theoretical and experimental project is a systematic investigation of collision induced processes in $H^+(H_2O)_n$ cluster cations. To achieve this ambitious goal, it is necessary to validate the employed methods at intermediate steps. As the key building block of $H^+(H_2O)_n$ clusters, the neutral H_2O molecule provides the starting point for our theoretical investigation. Systematic studies of small $H^+(H_2O)_n$ for $n = 1$–3 will be presented elsewhere. The first models developed here will describe the collision of an atom or ion with a H_2O molecule. As observables, we study the ionization and the motion of the various atoms in the system. In particular, we have explored the two limiting cases of low-velocity neutral and high-velocity charged projectiles for which one can reduce the dynamics to Born-Oppenheimer or pure electronic motion respectively. We have checked that our non-adiabatic method enables us to recover these limiting cases, as expected. In the present studies, we find that non-adiabatic effects do indeed remain negligible which *a posteriori* validates previous investigations. We thus focus on the cases of low-velocity charged and high-velocity neutral projectiles for which an accurate coupling between ionic and electronic dynamics becomes compulsory. We illustrate the capabilities of our approach on such cases.

4.2.1. Neutral atom impact upon H_2O at high-velocity

Fig. 2 shows results for a collision of a fast ($v = 0.1$–0.2 a.u.) neutral C atom with an H_2O molecule, for impact parameters b varying between 1.87 and 3.15 a_0 (these values are calculated with respect to the center of mass of the water molecule).

The water molecule lies in the scattering plane. The upper left panel shows the time evolution of ionization for impact velocity $v = 0.1$ a.u. $= 20\,a_0/\mathrm{fs}$ and different b. The sudden jump to $N_{esc} \approx 4$ is caused by the C atom leaving the numerical box and carrying its four active electrons away. The net ionization of the water molecule is the difference $N_{esc} - 4$. There is negligible ionization (and excitation) of the water molecule for the largest b (3.15 a_0). For $b = 2.21\,a_0$, however, we see a loss of about 0.2 charge units, whereas for the smallest b ($1.87a_0$) one full electron is lost. The reason for this becomes clear when we consider the right upper panel showing the trajectories in the scattering plane for the smallest impact parameter. The C atom travels from right to left through the box with negligible deviations from a straight line, first triggering ionization by about 0.2 charge units as shown in the left-hand panel. At the point of closest impact, the C atom hits one of the H atoms and transfers a sufficiently large momentum that the H atom dissociates from the molecule and leaves the box taking the attached 0.8 electrons away.

The lower right panel shows the trajectories for the impact parameter $b = 2.21a_0$. There is again a strong impact on the H atom closest to the projectile. As for the smaller impact parameter, there is still a significant ionization of about 0.2 charge units. However, the transferred momentum is sufficiently low that the atom remains bound in the molecule. The H atom rotates around the O atom and pushes the other H atom into the same rotation such that the structure of molecule is essentially conserved. Thus, in this case, atom impact has triggered strong rotational motion only.

Finally, the lower left panel shows ionization for medium impact parameter $b = 2.21\,a_0$ and two different velocities (0.1 and 0.2 a.u.). Ionization increases with velocity although the change is surprisingly small. We have here two counteracting influences. The faster atom exposes the molecule's higher frequency components so it can enhance ionization. On the other hand, the time of interaction becomes much shorter leading to a reduced reaction yield. The combination of these effects leads to a rather small velocity dependence in this range.

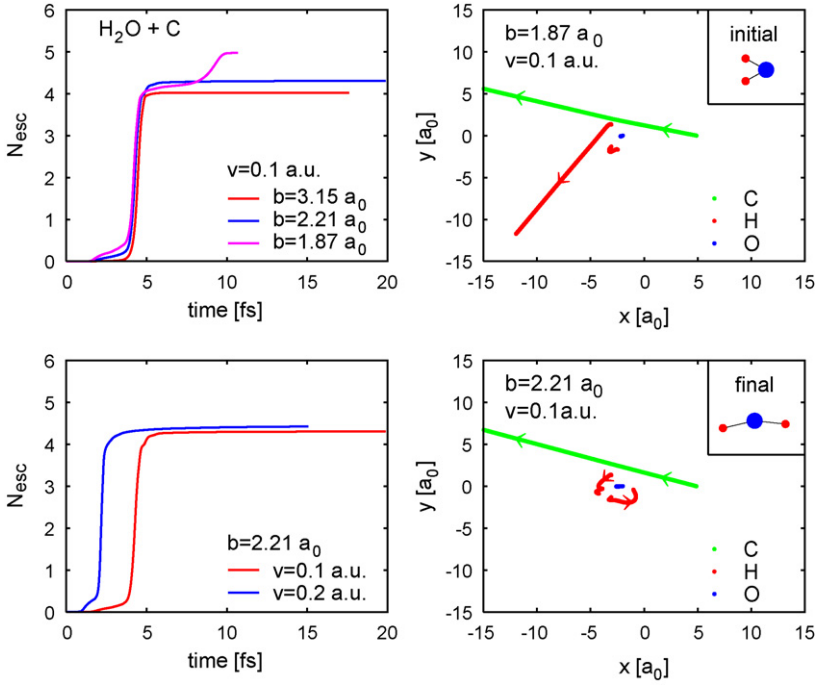

Fig. 2. Modeled collision between a water molecule and a C atom at various high velocities and impact parameters b. Left panels: number of escaped electrons as a function of time. Right panels: ionic trajectories in the x–y plane; the arrows indicate the time evolution; the insert in the top right panel shows the initial configuration of H_2O for all calculations, while that in the bottom right panel presents the final configuration only for the case $v = 0.1$ a.u. and $b = 2.21a_0$.

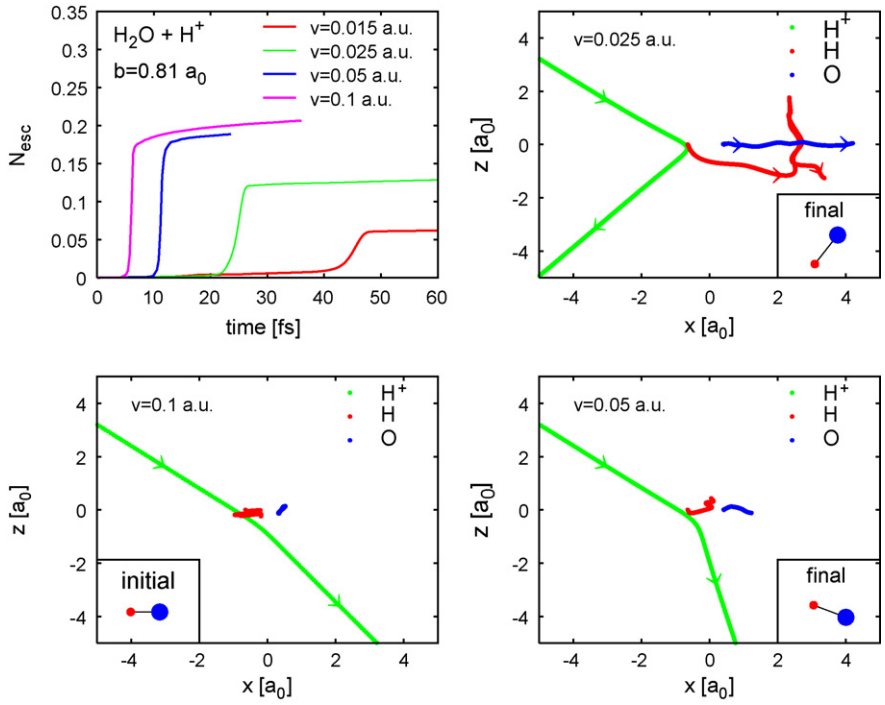

Fig. 3. Modeled collision between a water molecule and a H^+ ion at low velocities ($v = 0.015 - 0.1$ a.u.) for a fixed impact parameter $b = 0.81a_0$. Top left panel: number of escaped electrons as a function of time. Other panels: ionic trajectories in the x–z plane. The arrows indicate the time evolution; only in the top right panel, the arrows on the water molecule are drawn at same instant. The insert in the bottom left panel shows the initial configuration of H_2O for all the calculations, while the other inserts present the final configuration for $v = 0.05$ a.u. (bottom right) and $v = 0.025$ a.u. (top right).

4.2.2. Proton impact upon H_2O at low velocity

The calculations treating charged projectile H^+ collisions with H_2O at a small impact parameter ($b = 0.81a_0$) and at various low velocities are shown in Fig. 3. The H_2O molecule is placed with the O atom in the scattering plane and the two H atoms facing out of the plane. The interaction between the charged projectile and the molecule has a larger range than the neutral projectile case due to ion charge coupling with the large dipole moment of the water molecule. As a consequence, the projectile trajectories experience bending depending on the projectile velocity. The upper right panel shows the lowest velocity case and it is clear that the bending angle is very high. The water molecule as a whole is accelerated to a translational motion combined with some rotation of the two H atoms relative to the O atom (compare the initial and final configurations shown in the inserts). The lower right panel represents a collision at 0.05 a.u. The bending of the projectile trajectory and the effect on the motion of the H_2O molecule are both markedly smaller than observed for $v = 0.025$ a.u.. Again, the molecule is accelerated to translational motion with some small rotation, but this time in the other direction. The fastest collision is shown in the lower left panel. The much shorter interaction time reduces bending and impact on the molecule. The left upper panel shows ionization for the various impact velocities. The slowest collision, although having the largest effect on molecular motion, produces the least electron emission. Ionization increases with increasing velocity and seems to level off near the largest velocity. Thus, the enhancement by higher frequency components dominates over reduced interaction time in that (low) velocity range.

The theoretical test cases have demonstrated the feasibility of detailed dynamical simulations of water systems excited by various projectiles. We have seen a significant difference in the dynamics triggered by neutral (C atom) versus charged (H^+ ion) projectiles. There is sizeable impact ionization. The effects on the molecular motion as a whole are large and depend sensitively on the impact conditions.

5. Conclusion and outlook

In this paper, we have demonstrated the ability to produce intense beams of accelerated and size-selected water cluster ions in our newly constructed cluster/atom collision apparatus. The accompanying theoretical studies have demonstrated our ability to explore the dynamics of water systems irradiated by various projectiles. The next steps of the experimental investigation will focus on the effects of irradiation of size-selected water cluster ions. The parallel theoretical investigations are currently being extended to consider irradiation of small singly charged water clusters. In particular, comparisons will be drawn between our experimental and theoretic studies of size-selected water cluster ion collisions with high-velocity protons. Attachment of water molecules to a molecule of biological interest will constitute a further step both from the experimental and theoretical sides. The experimental capability to control the number of attached water molecules is essential for a direct comparison with theoretical calculations. This opportunity will be exploited in the studies to come.

Acknowledgments

This work was supported by the Deutsche Forschungsgemeinschaft (RE 322/10-1), the Humboldt foundation, a Gay-Lussac prize, Institut Universitaire de France, Agence Nationale de la Recherche (ANR-06-BLAN-0319-02), and the French computational facilities CalMip (Calcul en Midi-Pyrénées), IDRIS and CINES.

References

[1] W.F. Heidenreich, H.G. Paretzke, Radiat. Res. 170 (2008) 613.
[2] P. Jacob, Radiat. Res. 169 (2008) 602.
[3] F. Gobet, B. Farizon, M. Farizon, M.J. Gaillard, M. Carré, M. Lezius, P. Scheier, T.D. Märk, Phys. Rev. Lett. 86 (2001) 3751.
[4] G. Bruny, C. Montano, S. Feil, S. Eden, H. Abdoul-Carime, B. Farizon, M. Farizon, S. Ouaskit, and T.D. Märk, in preparation.

[5] F. Gobet, S. Eden, B. Coupier, J. Tabet, B. Farizon, M. Farizon, M.J. Gaillard, S. Ouaskit, M. Carré, T.D. Märk, Chem. Phys. Lett. 421 (2006) 68.
[6] D.W. Ledman, R.O. Fox, J. Am. Soc. Mass Spectrom. 8 (1997) 1158.
[7] S. Tomita, J.S. Forster, P. Hvelplund, A.S. Jensen, S.B. Nielson, Eur. Phys. J. D 16 (2001) 119.
[8] O. Echt, D. Kreisle, M. Knapp, E. Recknagel, Chem. Phys. Lett. 108 (1984) 401.
[9] V. Hermann, B.D. Kay, A.W. Castleman Jr., Chem. Phys. 72 (1982) 185.
[10] S.Y. Huang, C.D. Huang, B.T. Chang, C.T. Yeh, J. Phys. Chem. B 110 (2006) 21783.
[11] K. Mori, D. Asakawa, J. Sunner, K. Hiraoka, Rapid Commun. Mass Spectrom. 20 (2006) 2596.
[12] J. Kohanoff, E. Artacho, AIP Conf. Proc. 1080 (2008) 78.
[13] M.P. Gaigeot, R. Vuilleumier, C. Stia, M.E. Galassi, R. Rivarola, B. Gervais, M.F. Politis, J. Phys. B 40 (2007) 1.
[14] F. Calvayrac, P.-G. Reinhard, E. Suraud, Phys. Rev. B 52 (1995) 17056.
[15] K. Yabana, G.F. Bertsch, Phys. Rev. B 54 (1996) 4484.
[16] F. Calvayrac, P.-G. Reinhard, E. Suraud, C.A. Ullrich, Phys. Rep. 337 (2000) 493.
[17] E. Runge, E.K.U. Gross, Phys. Rev. Lett. 52 (1984) 997;
E.K.U. Gross, W. Kohn, Adv. Quant. Chem. 21 (1990) 255;
M.A.L. Marques, E.K.U. Gross, Ann. Rev. Phys. Chem. 55 (2004) 427.
[18] J.P. Perdew, Y. Wang, Phys. Rev. B 45 (1992) 13244.
[19] R. Car, M. Parinello, Phys. Rev. Lett. 55 (1985) 2471.
[20] W. Kohn, L.J. Sham, Phys. Rev. 140 (1965) 1133.
[21] R.M. Dreizler, E.K.U. Gross, Density Functional Theory: An Approach to the Quantum Many-Body Problem, Springer-Verlag, Berlin, 1990.
[22] A. Domps, P.-G. Reinhard, E. Suraud, Phys. Rev. Lett. 81 (1998) 5524.
[23] T. Fennel, G.F. Bertsch, K.-H. Meiwes-Broer, Eur. Phys. J. D 29 (2004) 367.
[24] F. Fehrer, P.-G. Reinhard, E. Suraud, E. Giglio, B. Gervais, A. Ipatov, Appl. Phys. A 82 (2006) 151.
[25] M. Bär, L.V. Moskaleva, M. Winkler, P.-G. Reinhard, N. Rösch, E. Suraud, Eur. Phys. J. D 45 (2007) 507.
[26] P.-G. Reinhard, E. Suraud, Introduction to Cluster Dynamics, Wiley, New York, 2003.
[27] C. Legrand, E. Suraud, P.-G. Reinhard, J. Phys. B 35 (2002) 1115.
[28] S. Goedecker, M. Teter, J. Hutter, Phys. Rev. B 54 (1996) 1703.
[29] M.D. Feit, J.A. Fleck, A. Steiger, J. Comp. Phys. 47 (1982) 412.
[30] G. Lauritsch, P.-G. Reinhard, Int. J. Mod. Phys. C 5 (1994) 65.